D'Angelo *et al. Clinical Epigenetics* (2026) 18:2
https://doi.org/10.1186/s13148-025-02024-6

Clinical Epigenetics

RESEARCH Open Access

Hypomethylation of the *MEG8*:Int2-DMR in patients with pathogenic *PLAG1* variants suggests new role of the chr14q32 imprinting cluster in Silver-Russell syndrome

Emilia D'Angelo[1], Laura Pignata[2], Francesco Cecere[1,3], Alessandro Vimercati[4], Maria Vittoria Cubellis[5], Abu Saadat[1], Carlo Giaccari[1,3], Nathalie Thibaud[6], Thomas Eggermann[7], Jose Ramon Fernández-Fructuoso[8], Silvia Russo[4], Irène Netchine[9], Flavia Cerrato[1], Andrea Riccio[1,3*] and Frédéric Brioude[9*]

Abstract

Background Silver-Russell syndrome (SRS) is a clinically and genetically heterogeneous imprinting disorder. The most common molecular defects are loss of methylation of the *H19/IGF2*:IG-DMR on chromosome 11p15.5, followed by maternal uniparental disomy of chromosome 7. Further molecular lesions are genetic variants in the *PLAG1* oncogene, as well as in the transcription factor *HMGA2* and the fetal growth factor *IGF2*. A phenotypic overlap exists between SRS and Temple syndrome (TS14) that is also characterized by growth restriction but associated with abnormalities in the imprinted chromosome 14q32 gene cluster. In TS14 patients, the germline *MEG3/DLK1*: IG-DMR is hypomethylated and the *MEG8*:Int2-DMR gains methylation probably as consequence of transcriptional readthrough from the *MEG3* promoter on the paternal chromosome. However, the functional role of the *MEG8* DMR remains unknown.

Results We analysed the DNA methylation of 11–12 imprinted regions in 17 cases with clinical SRS features and heterozygous for a *PLAG1* variant. We observed a specific loss of methylation of the *MEG8*:Int2-DMR in the ten cases carrying pathogenic *PLAG1* variants that result in stable aberrant proteins. Normal *MEG8* methylation was observed in the cases carrying variants of uncertain pathogenicity or gene deletions. Most of the *PLAG1* cases are familial and both epigenetic and genetic defects co-segregated within the families. Additionally, we assessed the methylation status of the *MEG8*:Int2-DMR in several SRS patients with *HMGA2* or *IGF2* variants, *H19/IGF2*:IG-DMR-LoM and upd(7)mat and all of them showed normal methylation.

Conclusions Our results indicate that pathogenic *PLAG1* variants leading to stable aberrant PLAG1 proteins and possibly acting in a dominant-negative manner influence methylation of the *MEG8* locus. This study suggests a new pathogenetic mechanism of the *PLAG1* gene in SRS, involving imprinted genes in the chr14q32 cluster through

*Correspondence:
Andrea Riccio
andrea.riccio@unicampania.it
Frédéric Brioude
frederic.brioude@aphp.fr

Full list of author information is available at the end of the article

deregulation of the *MEG8*:Int2-DMR and provides an epigenetic signature that may be used to assess the damaging potential of the *PLAG1* variants.

Keywords Silver-Russell syndrome, Growth retardation, Genomic imprinting, DNA methylation

Background

Imprinting disorders (ImpDis) are a group of congenital diseases caused by deregulation of imprinted genes and affecting human growth, metabolism and behaviour [1]. Most imprinted genes are organized in clusters, where their parent of origin-dependent expression is regulated by *cis*-acting regions exhibiting differential DNA methylation (Differentially Methylated Regions, DMRs) between the maternal and paternal alleles [2]. Imprinted DMRs are categorized into two groups: primary DMRs, also known as germline DMRs, and secondary DMRs, also referred to as somatic DMRs. Germline DMRs acquire their methylation pattern during gametogenesis and are stably maintained through the epigenetic reprogramming occurring during the oocyte-to-embryo transition. In contrast, somatic DMRs acquire their allele-specific methylation post-fertilization and are regulated by the neighbouring germline DMR in a hierarchical manner [3]. ImpDis are associated with genetic and epigenetic alterations involving changes in both gene sequences (genetic mutations) and gene regulation (epigenetic mutations) in imprinted gene clusters [1]. Epigenetic abnormalities can affect a single or multiple germline DMRs (multi-locus imprinting disturbances, MLID) and can be associated with genetic variants acting *in cis* or *in trans* [2, 4].

Silver-Russell syndrome (SRS; OMIM #180,860; prevalence at birth 1:30,000/1:100,000) is a clinically and genetically heterogeneous imprinting disorder, characterised by intrauterine and post-natal growth retardation, relative macrocephaly at birth, feeding difficulties, protruding forehead in early life and body asymmetry, along with numerous additional features at lower frequencies. According to the Netchine-Harbison clinical scoring system (NH-CSS), a clinical diagnosis is considered if a patient scores at least four out of six most frequent criteria [5]. However, the definition of Silver-Russell syndrome spectrum (SRSp) has been proposed to include cases with a clinical score < 4 yet still exhibiting clinical or molecular features of SRS [6]. Despite the complexity of its molecular mechanisms, an underlying molecular cause can currently be identified in around 60% of patients with clinical diagnosis of SRS. The most common molecular alterations are loss of methylation (LoM) at the *H19/IGF2*:IG (intergenic)-DMR, also known as IC1, on chr11p15.5, accounting for 30–60% of patients and maternal uniparental disomy of chromosome 7 (upd(7)mat) detected in 5–10% of the cases [5]. About 10–20% of SRS cases with IC1-LoM show MLID [7, 8]. Further molecular lesions associated with SRS phenotype are represented by genetic variants in *PLAG1* (*Pleiomorphic Adenoma Gene 1*), *IGF2* (*Insulin Like Growth Factor 2*), *HMGA2* (*High Mobility Group AT-Hook 2*) and more rarely *CDKN1C* (*Cyclin Dependent Kinase Inhibitor 1C*) gene [9–12].

A phenotypic overlap exists between SRS and Temple syndrome (TS14) that is also characterized by growth restriction but associated with abnormalities in the imprinted chr14q32 gene cluster (Fig. 1). This evolutionary conserved imprinted region contains the paternally expressed genes *DLK1, RTL1* and *DIO3* and the maternally expressed noncoding RNA genes *MEG3/GTL2, MEG8, MEG9,* and *RTL1AS*, as well as two large clusters of maternally expressed microRNAs (miRNAs) and small nucleolar RNAs (snoRNAs) [13]. The parent-of-origin-specific expression of the imprinted chr14q32 genes is regulated by two DMRs: the germline *MEG3/DLK1*:IG-DMR located between the *DLK1* and *MEG3* genes and the somatic *MEG3*:TSS-DMR overlapping the *MEG3* promoter region [14]. The *MEG3/DLK1*:IG-DMR acts upstream of the *MEG3*:TSS-DMR and governs it in a hierarchical fashion [15, 16]. Two further somatic DMRs have been recently described, the *MEG8*:Int2-DMR located in intron 2 of the *MEG8* gene and the *DLK1*:Int1-DMR overlapping the second exon of the *DLK1* gene [17–19]. The function of these two DMRs is currently unknown. In TS14 patients, the paternally methylated *MEG3/DLK1*:IG-DMR and *MEG3*:TSS-DMR are hypomethylated leading to upregulation of *MEG3* and *MEG8* and downregulation of *DLK1*. In these cases, the *MEG8*:Int2-DMR, normally methylated on the maternal chromosome, gains methylation probably as consequence of transcriptional readthrough derived from the activated paternal *MEG3* promoter [17]. The overlapping phenotypic features between SRS and TS14 can be attributed to the involvement of shared biological pathways and/or gene co-regulation [1]. Several trans-molecular interactions between imprinted genes located on chr11p15 and chr14q32 have been reported. In particular, the concomitant overexpression of *MEG3* and *MEG8* leads to downregulation of *IGF2* in cultured cells [20].

PLAG1, located on human chromosome 8q12, was initially identified as an oncogene associated with certain types of cancer and is the main translocation target in pleomorphic adenomas of the salivary glands [21]. It belongs to the PLAG family of zinc finger transcription factors, along with PLAG-like 1 (PLAGL1), which is a tumor suppressor, and PLAG-like 2 (PLAGL2), which

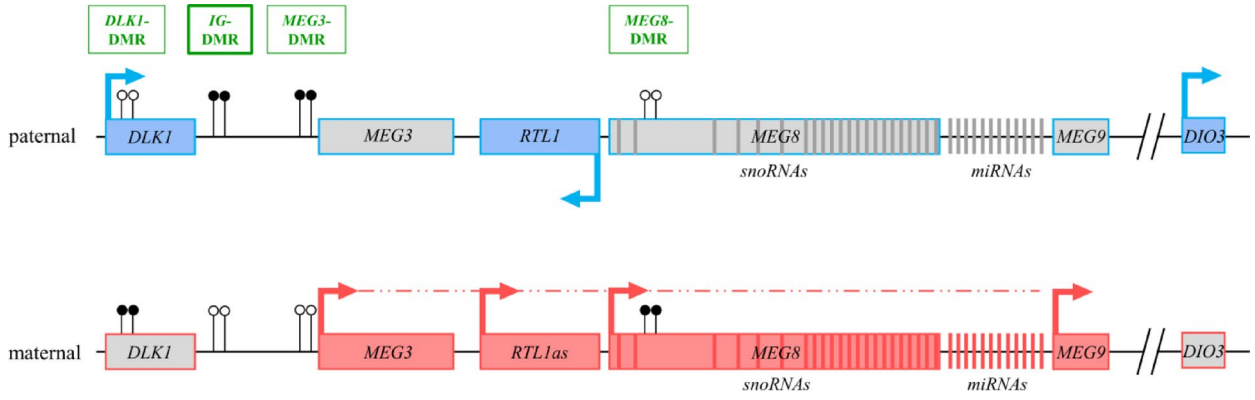

Fig. 1 Schematic representation of the imprinted gene cluster on human chromosome 14q32. Paternally expressed genes are shown in light blue, while maternally expressed genes are represented in red. DNA methylation is indicated by black lollipops. The IG-DMR (*MEG3/DLK1*: IG-DMR) and the *MEG3*-DMR (*MEG3*: TSS-DMR) are methylated on the paternal allele, whereas the *DLK1*-DMR (*DLK1*:Int1-DMR) and the *MEG8*-DMR (*MEG8*:Int2-DMR) are methylated on the maternal allele. The dashed red line represents the maternally expressed polycistronic transcript starting from the *MEG3* promoter

acts as an oncogene. PLAG1 protein contains seven canonical C2H2 zinc finger domains (ZF) and a serine-rich COOH terminus that exhibits transactivation capacities suggesting that it may act as a transcriptional regulator. Its DNA binding site is composed of the core sequence GRGGC and a G-cluster RGGK separated by seven random nucleotides. The interaction with the core sequence is mediated by fingers 6 and 7, and that with the G-cluster by finger 3 [22]. The three PLAG proteins share the highest degree of homology in their NH_2-terminal zinc finger domain, with PLAGL1 and PLAGL2 showing 73% and 79% identity, respectively. In contrast, the COOH-terminal region is significantly more divergent. The greatest similarity is observed in zinc fingers 6 and 7, suggesting that PLAGL1 and PLAGL2 may also recognize a core motif similar to the PLAG1 core (GRGGC). Zinc fingers 2–5 are less conserved, but key amino acids at critical positions remain preserved [21, 22]. PLAGL1 dimerization through zinc finger 2 enhances transactivation of target genes, suggesting that also PLAG1 may act as a dimer [23].

PLAG1 plays a critical role in the oncogenic *HMGA2–PLAG1–IGF2* pathway as it has been shown to be a transcriptional activator of *IGF2* that binds its P3 promoter [22]. Genetic defects of this pathway can lead to fetal and postnatal growth restriction [10]. Inherited or de novo alterations involving the *PLAG1* gene, including whole-gene deletions and intragenic pathogenic variants, were demonstrated in several cases with phenotypic features of SRS [10, 11, 24–33]. It has been proposed that *PLAG1* haploinsufficiency leads to *IGF2* repression and growth deficiency [10]. However, if further genes have a role in mediating the effect of *PLAG1* on somatic growth is unknown.

To look for a possible dysregulation of imprinted genes linked to *PLAG1* defects, we analysed the DNA methylation of 11–12 imprinted regions in 17 cases with clinical SRS features carrying heterozygous *PLAG1* variants. We observed loss of methylation of the *MEG8*:Int2-DMR in all the cases predicted to generate stable aberrant PLAG1 proteins, but not in those with whole gene deletions, VUS or protein variants with C-degron recognized by APPBP2, indicating a functional interaction between PLAG1 and the chr14q32 imprinting cluster.

Patients

The study cohort included 17 patients with clinical diagnosis of SRS based on the Netchine-Harbison clinical scoring system (Additional file 1: Table S1). In these patients IC1 LoM and upd(7)mat as well as molecular TS14 were excluded. As detailed in Table 1, 8 cases were reported in previous publications. All the cases carried a variant involving the *PLAG1* gene. In addition, 54 age-matched control samples were included for comparison. This control group consisted of unrelated individuals with no clinical features of the syndrome, analysed following the same molecular conditions as the patient cohort. The group comprised both Italian and French individuals.

Materials and methods

DNA extraction

Genomic DNA of patients and their relatives was isolated from peripheral blood leukocytes (PBL) by standard procedures.

NGS analysis

For SRS3-SRS5, SRS10-SRS12 and their relatives, sequencing analysis has been reported previously [10, 25, 32, 33]. Specifically, for SRS3 and SRS4 library preparation, exome capture, sequencing, and data analysis were performed by IntegraGen SA (Evry, France). For SRS5 DNA was enriched using the Nextera Rapid Capture Exome (v.1.2) (Illumina, San Diego,

Table 1 Summary of the molecular features of the probands and their families

Cases	Proband sex	*PLAG1* variant	Pathogenicity evaluation*	Genotype	*MEG8*:Int2-DMR methylation	Clinical features of proband	Publication
SRS1	Female	NM_002655.3: c.1023 T > A; p.Tyr341* novel nonsense mutation	Likely pathogenic	Proband: het Mother: het Father: wt	Proband: hypomethylation Mother: hypomethylation Father: NA	NH-CSS: 4/6 Small for gestational age, post-natal growth retardation, microcephaly, low body mass index, no protruding forehead	This study
SRS2	Female	NM_002655.3: c.527C > A; p.Ser176* novel nonsense mutation	Likely pathogenic	Proband: het Mother: wt Father: wt	Proband: hypomethylation Mother: normal methylation Father: NA	NH-CSS = 3/6 Small for gestational age, post-natal growth retardation, feeding difficulties during infancy, head circumference (– 1.5 SDS) but no values available	This study
SRS3	Female	NM_002655.2: c.1363del; p.Gln455Serfs*16 novel frameshift mutation-premature stop	Likely pathogenic	Proband: het Mother: wt Father: wt	Proband: hypomethylation Mother: NA Father: NA	NH-CSS = 4/6 Small for gestational age, feeding difficulties during infancy, prominent forehead with triangular face, relative macrocephaly at birth	Abi Habib W et al. [10]
SRS4	Female	NM_002655.2: c.439del; p.Ser147Valfs*82 novel frameshift mutation-premature stop	Pathogenic	Proband: het Mother: het Father: wt Proband's sister: het	Proband: hypomethylation Mother: hypomethylation Father: NA Proband's sister: hypomethylation	NH-CSS = 4/6 Small for gestational age, postnatal growth failure, feeding difficulties during infancy, prominent forehead with triangular face	Abi Habib W et al. [10]
SRS5	Female	NM_002655.2: c.599dup; p.Arg201Profs*52 novel frameshift mutation-premature stop	Likely pathogenic	Proband: het Mother: wt Father: wt	Proband: normal methylation Mother: NA Father: NA	NH-CSS = 4/6 Small for gestational age, postnatal growth retardation, feeding difficulties during infancy, prominent forehead	Meyer R., et al., [25]
SRS6	Female	NM_002655.3: c.666del; p.Phe222Leufs*7 novel frameshift mutation-premature stop	Likely pathogenic	Proband: het Mother: NA Father: NA	Proband: hypomethylation Mother: NA Father: NA	NH-CSS: 4/5 Small for gestational age, post-natal growth retardation, relative macrocephaly, feeding difficulties during infancy, protruding forehead noticed at the age of 3y4m	This study
SRS7	Male	NM_002655.3: c.779_780del; p.Val260Alafs*16 novel frameshift mutation-premature stop	Likely pathogenic	Proband: het Mother: het Father: wt	Proband: hypomethylation Mother: hypomethylation Father: normal methylation	NH-CSS = 4/6 Small for gestational age, postnatal growth failure, feeding difficulties during infancy, prominent forehead with triangular face	This study
SRS8	Male	NM_002655.3: c.770del; p.Asn257Metfs*6 novel frameshift mutation-premature stop	Likely pathogenic	Proband: het Mother: het Father: wt	Proband: hypomethylation Mother: hypomethylation Father: normal methylation	NH-CSS = 3/5 Small for gestational age, postnatal growth retardation, triangular face with prominent forehead	This study
SRS9	Female	NM_002655.3: c.1455_1502del; p.Ser485delinsArgAspSerGlyThrTrpIleHisTyrArgAsnValCysValAlaValPro* novel stop-loss mutation; Change of the C-ter end of the peptide, elongated protein (+ 1 aa)	Likely pathogenic	Proband: het Mother:het Father:wt Proband's brother: het	Proband: hypomethylation Mother: hypomethylation Father: normal methylation Proband's brother: hypomethylation	NH-CSS = 4/6 Small for gestational age, postnatal growth failure, feeding difficulties during infancy, prominent forehead with triangular face	This study

Table 1 (continued)

Cases	Proband sex	*PLAG1* variant	Pathogenicity evaluation*	Genotype	*MEG8*:Int2-DMR methylation	Clinical features of proband	Publication
SRS10	Male	NM_002655.3: c.610_612del; p.Met204del novel in-frame deletion	Likely pathogenic	Proband: het Mother: het Father: wt	Proband: hypomethylation Mother: hypomethylation Father: normal methylation	NH-CSS = 4/6 Small for gestational age, postnatal growth failure, feeding difficulties during infancy, relative macrocephaly, triangular face	Vimercati A. et al.[23]
SRS11	Male	NM_002655.3: c.671G > A; p.(Arg224Gln) novel missense mutation	Likely pathogenic	Proband: het Mother: het Father: wt	Proband: hypomethylation Mother: hypomethylation Father: normal methylation	NH-CSS = 4/6 Small for gestational age, postnatal growth failure, feeding difficulties during infancy, triangular face with protruding forehead	Vimercati A. et al. [23]
SRS12	Male	NM_002655.3: c.545A > T; p.Glu182Val novel missense mutation	VUS Low Pathogenic Support	Proband: het Mother: NA Father: NA	Proband: normal methylation Father: NA Mother: NA	NH-CSS = 3/5 Post-natal growth retardation, feeding difficulties during infancy, prominent forehead	Kessler L et al. [32]
SRS13	Male	NM_002655.3: c.1162A > G; p.Ile388Val rs765459935 AF: 0.00001593 missense mutation	VUS > > cl2 Uncertain pathogenicity	Proband:het Mother:het Father:NA	Proband: normal methylation Mother: normal methylation Father: NA	NH-CSS = 2/6 Small for gestational age, postnatal growth retardation, low body mass index, microcephaly, hypospadias	This study
SRS14	Female	NM_002655.3: c.-117-5del p.? rs1023307529 AF: 0.0005235 non-coding; (intron–exon boundary)	VUS > > cl2 Uncertain pathogenicity	Proband: het Mother: het Father: wt Maternal grandmother: het Maternal grandfather: wt	Porband: normal methylation Mother: normal methylation Father: NA Maternal grandmother: NA Maternal grandfather: NA	NH-CSS = 4/6 Small for gestational age, postnatal growth retardation, protruding forehead, feeding difficulties during infancy	This study
SRS15	Female	chr8q12.1 deletion including the *PLAG1* gene arr [GRCh37] 8q12.1 (56,834,331_ 58,921,491) × 1	Pathogenic	Proband: het Mother: wt Father: wt	Proband: normal methylation Father: NA Mother: NA	NH-CSS = 4/6 Small for gestational age, moderate postnatal growth retardation, feeding difficulties during infancy, relative macrocephaly, triangular face	Fernández-Fructuoso JR. et al. [27]
SRS16	Male	chr8q12.1 deletion including the *PLAG1* gene arr [GRCh37] 8q12.1 (57,079,399_57,155,945) × 1	Pathogenic	Proband: het Mother: wt Father: wt	Proband: normal methylation Father: NA Mother: NA	NH-CSS = 2/6 Feeding difficulties during infancy, triangular face with prominent forehead	Baba N et al. [28]
SRS17	Male	chr8q12.1 deletion including the *PLAG1* gene arr[GRCh37]8q12.1 (56,986,129_57,169,684) × 1	Pathogenic	Proband:het Mother:wt Father:wt	Proband: normal methylation Father: NA Mother: NA	NH-CSS = 4/6 Small for gestational age, postnatal growth retardation, low body mass index, relative macrocephaly at birth (but not after birth)	This study

*Pathogenicity assessment based on ACMG criteria. In third column AF: Allele frequency in European population. In fifth column: het = heterozygous; wt = wild type. In both fifth and sixth column: NA = not analysed

CA, USA). Sequencing was performed using a NextSeq500 Sequencer (Illumina, San Diego, CA, USA). Targeted sequencing was carried out for cases SRS10 and SRS11. Libraries were prepared using the Nextera XT DNA Library Prep Kit (Illumina, San Diego, CA) and sequenced with an Illumina Miseq sequencer. For patient SRS12, genome sequencing (GS) was conducted by using the DNA PCR-free kit (Illumina Inc. San Diego, CA, USA) and sequencing was performed on a NovaSeq 6000 System (S4 Reagent Kit v1.5) (Illumina Inc.).

For SRS1, SRS2, SRS6, SRS13, SRS14 families, library preparation was performed using a custom sequencing panel designed by Sophia Genetics. Libraries were sequenced on a MiSeq (Illumina, San Diego, CA, USA).

For SRS7-SRS9 families, library preparation of single samples was performed using the SureSelect QXT Clinical Research exome v2 and Human All Exon V7 kits compatible with Illumina platform version F0(Agilent Technologies, Santa Clara, CA, USA) following the manufacturer's instructions. Libraries were sequenced using a NovaSeq6000 system (Illumina, San Diego, CA, USA) [34]. The WES data preprocessing followed the nf-core Sarek pipeline (version 3.3.2) using its default settings [35]. The sequencing reads were mapped to the human reference genome GRCh38 using the BWA-MEM algorithm. The resulting variant call format (VCFs) files were then annotated with Franklin by Genoox.

Validation and segregation analysis of variants in the family members were performed by Sanger sequencing.

Molecular karyotyping

Molecular karyotyping for SRS15 and SRS16 was previously reported [27, 28]. For SRS17, Comparative Genomic Hybridization (CGH) array analysis was carried out by using a 180 k microarray (Agilent Technologies, Santa Clara, CA, USA). Raw data were analysed by the CytoGenomics V3.0 software (Agilent Technologies).

In silico prediction of variant pathogenicity and protein stability

Variants were initially classified based on their predicted impact on the protein. In silico pathogenicity prediction was performed for all Single Nucleotide Variants (SNVs) and indels using CADD v1.7 [36]. For missense variants, additional analyses were conducted using PolyPhen-2 [37], SIFT [38], AlphaMissense [39] and REVEL [40]. Furthermore, all variants, including the three large deletions, were classified according to the ACMG standards and guidelines [41, 42]. Protein stability was investigated using DEGRONOPEDIA [43], which enables the identification of known degron motifs involved in protein degradation pathways.

Methylation analysis

Methylation-specific multiple ligation-dependent probe amplification (MS-MLPA) targeting 11 or 12 imprinted loci was performed using the SALSA MS-MLPA Kit (MRC-Holland, Amsterdam, The Netherlands) according to the manufacturer's instructions. Probemix ME034-C1 or Probemix ME034-D1, designed for multi-locus imprinting analysis, were used. Raw data were analysed using Coffalyser.Net software (MRC Holland, Amsterdam, The Netherlands). Pyrosequencing analysis was carried out as described in Sparago et al. [44] and it was conducted in separate batches of experiments. The 13 analysed CpGs are included in the following coordinates: chr14:100,904,601–100,904,702 (GRCh38/hg38). ImprintCap, a NGS-based methodology for large-scale methylation studies at several imprinted loci was performed as described in Brioude et al. [45] on 13 control samples to explore the methylation of *MEG8*:Int2-DMR. The 42 analysed CpGs are included in the following coordinates: chr14: 100,904,423- 100,905,080 (GRCh38/hg38).

Results

DNA methylation analyses

We investigated the DNA methylation of 11–12 imprinted regions in 17 SRS cases carrying rare *PLAG1* variants in heterozygosity (Table 1) and 54 control individuals, by using the multi-locus MS-MLPA C1 or D1 kit. Compared to the mean of the controls, we found a partial loss of methylation of the *MEG8*:Int2-DMR in the cases SRS1-SRS4,SRS6-SRS11 and SRS16. Most of these cases were familial and the imprinting defect segregated within the family, being detected in all the members who carried the *PLAG1* variant (Fig. 2). Conversely, *MEG8*:Int2-DMR methylation was normal in SRS5, SRS12-SRS15 and SRS17. The MS-MLPA results are reported in the Additional file 1: Table S2. In all cases, the methylation levels of the other tested DMRs, including the *MEG3*: TSS-DMR, were comparable to those of the controls (Fig. 2). In addition, we evaluated the methylation status of the *MEG8*:Int2-DMR in 7 SRS patients carrying *HMGA2* variants and 8 with *IGF2* variants and all of them showed normal methylation (Additional file 1: Table S3).

To further explore *MEG8* methylation in other molecular subgroups of SRS, we performed multi-locus MS-MLPA in 28 patients with IC1 loss of methylation (IC1-LoM), 4 with maternal uniparental disomy of chromosome 7, and 31 idiopathic cases (NH-CSS ≥ 4). All of these also exhibited normal methylation levels (Additional file 1: Table S4). Finally, 2/54 of the healthy control individuals showed lower methylation levels at the *MEG8*:Int2-DMR, according to the MS-MLPA results (Additional file 1: Table S5).

To validate the MS-MLPA results, we analysed *MEG8*:Int2-DMR methylation through the more quantitative pyrosequencing assay in the patients carrying the *PLAG1* variants and in several controls. With this assay, we tested the methylation level of 13 CpGs across the *MEG8*:Int2-DMR. The results were consistent with the data obtained by MS-MLPA in 10/11 patients and confirmed the co-segregation of the *MEG8*:Int2-DMR hypomethylation with the *PLAG1* variants (Fig. 3A–G).

Furthermore, the pyrosequencing results demonstrated that the hypomethylation affected the entire *MEG8*:Int2-DMR. The reduction in methylation levels was between 15 and 33% compared to the mean of the controls (Additional file 1: Table S6; Additional file 2: Fig. S1). Patient SRS16 and the two healthy individuals found hypomethylated with MS-MLPA showed a more modest (3–6%)

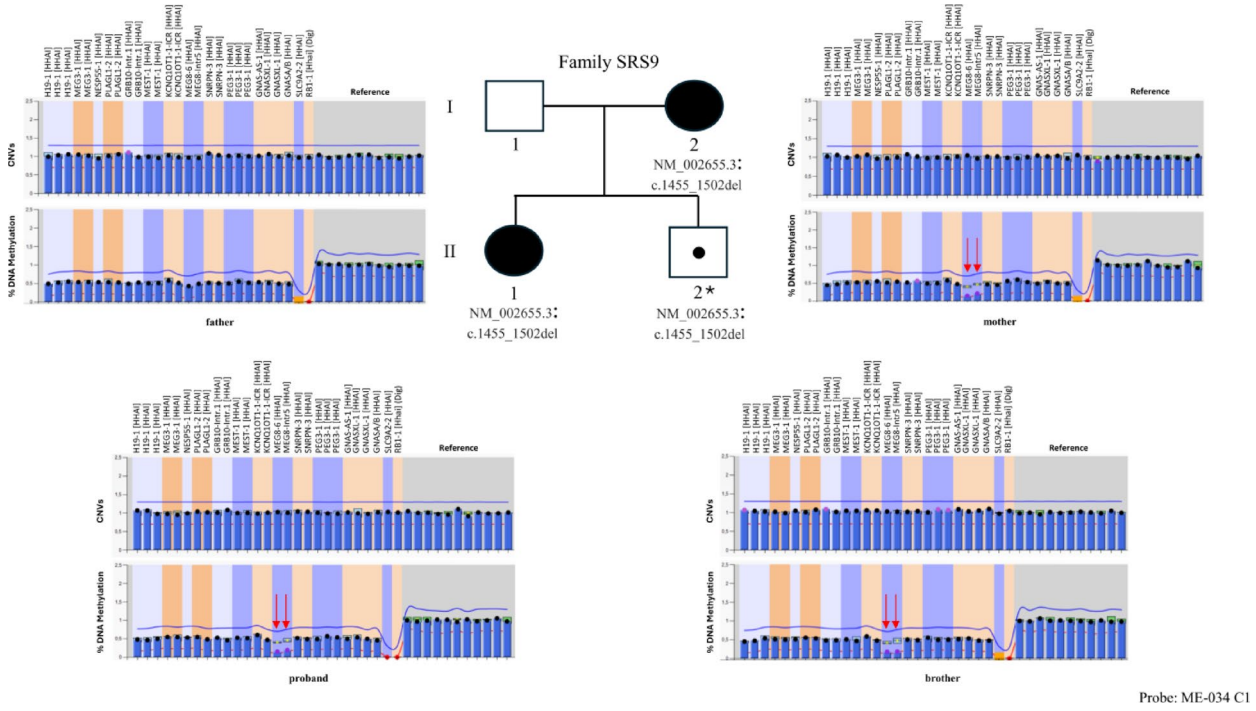

Fig. 2 Representative MS-MLPA results in one of the families. Copy number and DNA methylation were analysed for each member of the family SRS9 by ME034-C1 multilocus kit. The mean values of control subjects were used for assessment of relative copy number and methylation percentage. Red arrows indicate the probes detecting the methylation defect. *No clinical information was available for this patient

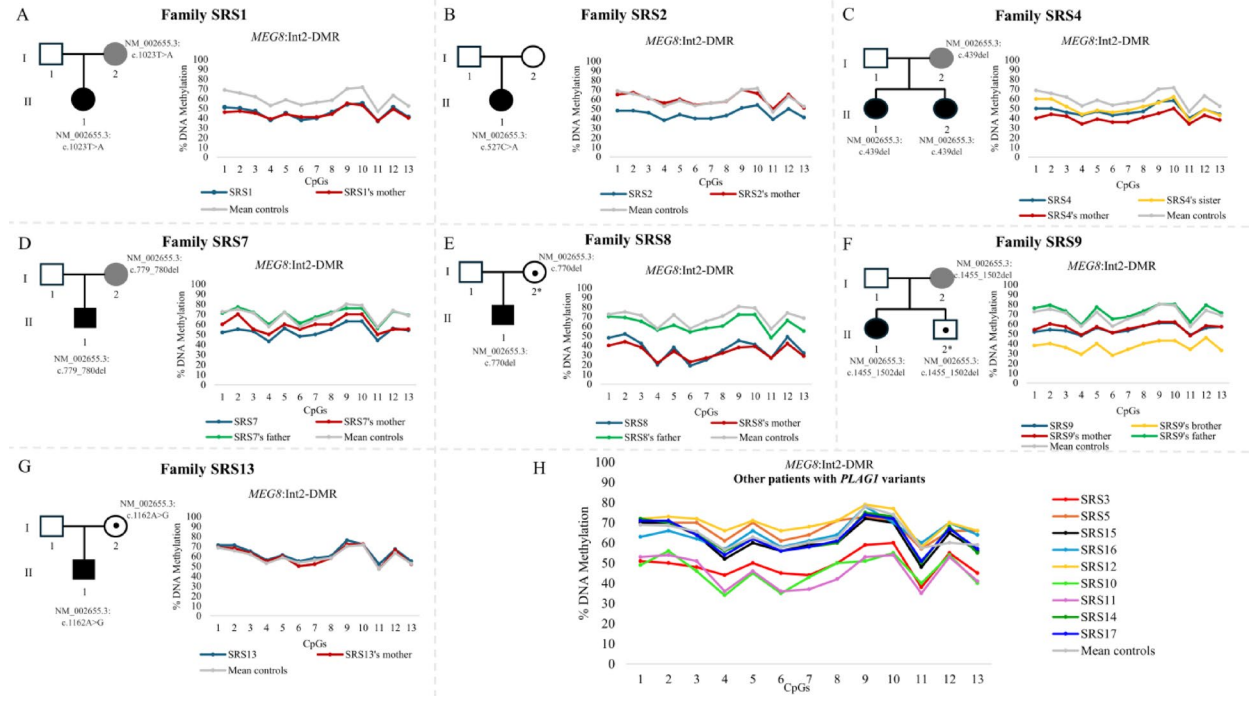

Fig. 3 Pyrosequencing analyses of DNA methylation at the *MEG8*:Int2-DMR in cases with 677 *PLAG1* variants. H shows data from additional patients (SRS3, SRS5, SRS10-SRS12, SRS14-SRS17) for whom no family member analysis was possible. DNA of patient SRS6 was not available for pyrosequencing analysis. The exact genomic positions of the 13 CpGs analysed are provided in Additional file 1: Table S6. Gray-background symbols indicate individuals with a milder phenotype; while symbols with black dots indicate that those individuals are carriers of the genetic variant although their clinical phenotype remains unclear. *No clinical information

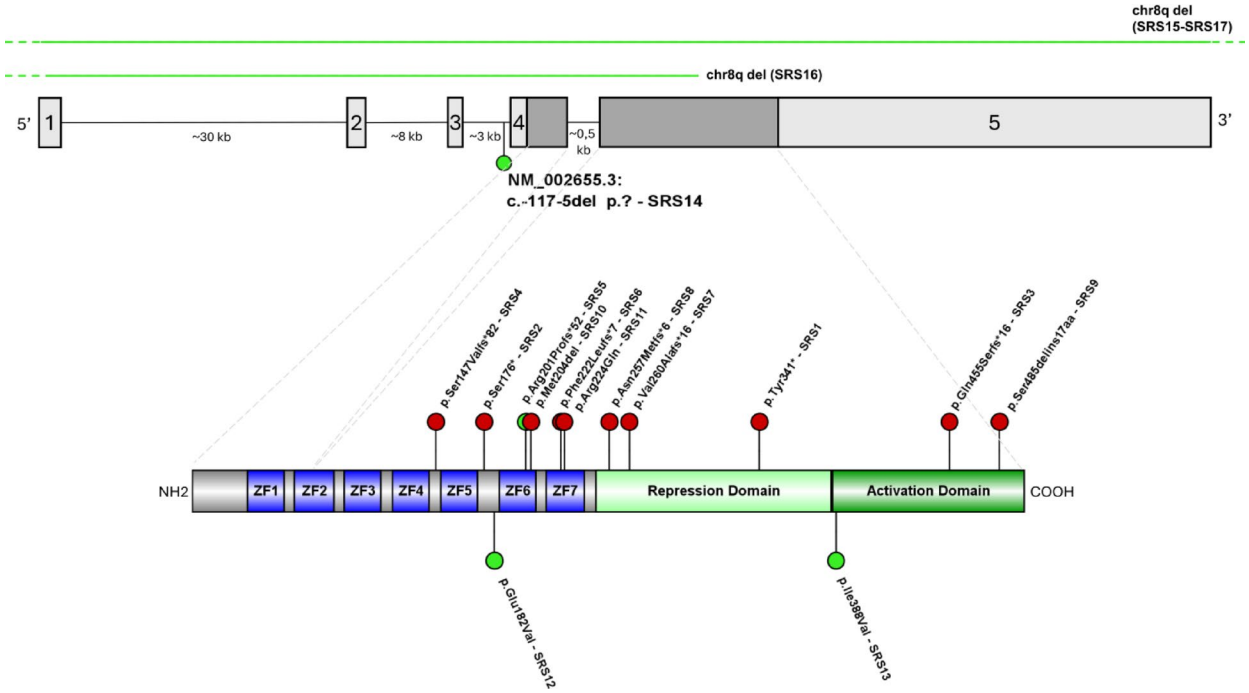

Fig. 4 *PLAG1* mutations. The top panel shows the exon/intron structure of the *PLAG1* gene, with exons 4 and 5 containing the coding sequences (highlighted in dark grey). The bottom panel illustrates the PLAG1 protein, with seven zinc fingers (ZF1-ZF7) represented in blue. Red lollipops indicate the variants associated with hypomethylation at the *MEG8*:Int2-DMR, while green lollipops denote the variants associated with normal methylation. The green upper lines highlight three cases with chr8q deletions encompassing the *PLAG1* gene, which are associated with normal methylation at the *MEG8*:Int2-DMR

methylation defect restricted to only a few CpGs located at the 5' part of the DMR (Fig. 3H; Additional file 1: Table S7; Additional file 3: Fig. S2). From ImprintCap analysis on 13 control samples, those latter 5'-CpGs were shown to be highly variable, making those 5'-CpGs not suitable to define gain or loss-of-methylation in patients (Additional file 1: Table S8; Additional file 4: Fig. S3).

In summary, these results indicate a specific loss of methylation of the entire *MEG8*:Int2-DMR in 10 out of 17 SRS cases carrying a genetic variant in *PLAG1.*

Genetic alterations in PLAG1

Since the *MEG8* methylation defect was not consistently present in all the 17 SRS cases with *PLAG1* variants, we assessed the pathogenic potential of the identified genetic variants by in silico analysis (Table 1). Figure 4 shows all the variants identified in our cohort. The clinical features and *PLAG1* variants of 8 patients (SRS3-SRS5, SRS10-SRS12 and SRS15, SRS16) have been described in previous studies [10, 25, 27, 28, 32, 33], while the remaining nine are novel cases.

The patients SRS1-SRS11 (Table 1) carried heterozygous SNVs or indels of *PLAG1* that were classified as pathogenic or likely pathogenic according to the ACMG guidelines and gene variant interpretation (Additional file 1: Table S9). In particular, two nonsense variants were identified in cases SRS1 and SRS2. The variant p.Tyr341* resulting in loss of the C-terminal activation domain was found in both the SRS1 proband and her mother, while the variant p.Ser176* causes the loss of ZF6, ZF7 and the entire C-terminal region of *PLAG1* in patient SRS2. Frameshift variants were identified in the cases SRS3-SRS8. These pathogenic variants lead to putative truncated proteins lacking key functional domains (Additional file 5: Fig. S4). In particular, the variant p.Gln455Serfs*16 identified in SRS3 results in a truncated protein with 496 amino acids [10]. The p.Ser147Valfs*82 mutation found in SRS4 causes a frameshift before the ZF5 domain, generating an abnormal peptide of 227 residues [10]. In patient SRS5, the p.Arg201Profs*52 variant leads to a truncated protein of 251 amino acids [25]. Additionally, the p.Phe222Leufs*7 mutation carried by patient SRS6 causes a frameshift starting from ZF7 and likely results in a truncated peptide composed of 227 amino acid residues (221 wild-type and 6 mutated), while the p.Val260Alafs*16 and p.Asn257Metfs*6 variants, inherited maternally by the SRS7 and SRS8 patients, respectively, lead to loss of the entire C-terminal domain, producing abnormal proteins of 274 and 261 amino acids. Notably, all the truncating variants occur in the last two exons of *PLAG1.*A novel 48 bp deletion was identified in the SRS9 proband, as well as in her mother and brother, but not in her father. This mutation likely results in a protein of 501 amino acids, with 484 wild-type, 16

mutated and one additional residue at the C-terminus (p.Ser485delinsArgAspSerGlyThrTrpIleHisTyrArgAsnValCysValAlaValPro*). Finally, SRS10 and SRS11 carried an in-frame deletion and a missense mutation in the ZF6 and ZF7 sequences, respectively [33].

To assess the stability of the 11 predicted aberrant proteins resulting from deleterious *PLAG1* mutations, we analysed the presence of known degron motifs involved in degradation pathways [43]. Notably, a RxxGxx motif was identified at the C-terminus of the PLAG1 mutant p.Arg201Profs*52 (SRS5). APPBP2, a substrate receptor of CRL2 (Cullin-RING E3 ubiquitin ligase 2) complexes, is known to recognize C-degrons defined by a distinctive C-terminal Arg-x-x-Gly sequence [46]. This specific degron motif was absent in the other mutated proteins that were subjected to analysis, suggesting a potential importance of the R-x-x-G motif in substrate recognition and subsequent ubiquitination processes within CRL2-mediated proteolysis for the PLAG1 mutant p.Arg201Profs*52 (Additional file 5: Fig. S4).

According to the results of the in-silico analysis and the ACMG criteria, the patients SRS12 [32], SRS13 and SRS14 carried Variants of Uncertain Significance (VUS) in the *PLAG1* gene (Table 1, Additional file 1: Table S9). In particular, an intronic variant (NM_002655.3:c.-117-5del;p.?) occurring in a homopolymeric region of *PLAG1* intron 3 was found in SRS14, her mother and her healthy maternal grandmother, while the missense variants p.Glu182Val and p.Ile388Val were identified in cases SRS12 and SRS13, respectively. In particular, the p.Ile388Val variant involved a non-conserved residue and, in both SRS12 and SRS13 cases, the functional *PLAG1* domains were not affected. Thus, their pathogenicity remains uncertain.

Finally, patients SRS15 [27], SRS16 [28], and SRS17 carried heterozygous deletions on chromosome 8q (Table 1; Additional file 6: Fig. S5). Among them, patient SRS16 exhibited the smallest deletion, affecting only *PLAG1* and *CHCHD7* genes. In contrast, SRS15 presented with a larger de novo deletion of approximately 2.1 Mb at 8q12, encompassing 32 genes, including 9 OMIM-annotated genes. In SRS17, molecular karyotyping identified a ~ 183 kb de novo deletion (arr[GRCh37]8q12.1(56,986,129_57,169,684) × 1) involving *PLAG1* but also *CHCHD7, MOS,* and *SDR16C5*. In all three cases, *PLAG1* was proposed as the primary candidate gene responsible for the observed SRS phenotype [27, 28]. According to the ACMG criteria, all three deletions are classified as pathogenic.

Overall, we collected a wide spectrum of *PLAG1* variants: two nonsense variants (SRS1-SRS2), six frameshift (SRS3-SRS8), one stop-loss (SRS9), one in-frame deletion (SRS10), three missense variants (SRS11-SRS13), one intronic variant (SRS14), and three large deletions (SRS15-SRS17) affecting the entire *PLAG1* gene on chromosome 8q. Evaluation of their potential pathogenicity led us to observe that 11 out of 14 SNVs/indels were predicted to be damaging, whereas the remaining 3 were classified as VUS. Among these 11 damaging variants, one harbours a degron motif likely associated with protein degradation. The copy number variants were also classified as pathogenic.

Correlation of MEG8 methylation with PLAG1 gene variants

To further investigate the relationship between *MEG8*:Int2-DMR methylation and PLAG1 function, we compared the methylation of this locus among the 17 SRS patients carrying different *PLAG1* variants (Table 1). Interestingly, loss of *MEG8*:Int2-DMR methylation was detected in 10 out of 11 cases carrying pathogenic or likely pathogenic single nucleotide variants or indels, with SRS5 (p.Arg201Profs*52) representing the only exception. In particular, this mutated protein uniquely harbours the C-terminal RxxGxx motif, which facilitates protein degradation [46, 47], suggesting a distinct impact on protein stability compared with the other pathogenic mutations. Conversely, all the 6 cases carrying VUS or large deletions encompassing the *PLAG1* gene showed normal methylation levels. Notably, *MEG8*:Int2-DMR hypomethylation was not detected in any of the SRS patients with molecular alterations in other genes of the *HMGA2–PLAG1–IGF2* pathway, in those with IC1-LoM, upd(7)mat and in idiopathic SRS cases.

In summary, *MEG8* hypomethylation is associated with *PLAG1* variants that are predicted to produce stable abnormal proteins, but not with whole *PLAG1* gene deletions, variants of uncertain pathogenicity or variants leading to protein degradation.

Discussion

The observed association between damaging *PLAG1* variants and *MEG8*:Int2-DMR hypomethylation in SRS indicates a possible role of *PLAG1* in regulating the expression of chr14q32 imprinted genes controlling somatic growth.

In the present study, *MEG8*:Int2-DMR hypomethylation was demonstrated in cases with pathogenic or likely pathogenic *PLAG1* variants that are predicted to produce abnormal proteins. In contrast, normal *MEG8* methylation was observed in the cases with missense/intronic variants classified as VUS according to the ACMG guidelines and *PLAG1* deletions. In addition, most of the pathogenic *PLAG1* cases are familial and both epigenetic and genetic defects co-segregated within the families, further supporting the association between damaging *PLAG1* variants and *MEG8* hypomethylation. This epigenetic defect appears to be specific for *PLAG1*, because it was not found in the cases with *HMGA2* and

IGF2 variants, patients with IC1-LoM, upd(7)mat cases and idiopathic cases.

Apart from *MEG8*, the methylation of other 10–11 imprinted loci was found to be normal in the patients studied, suggesting a specific interaction between PLAG1 and *MEG8*-DMR. Analysis of chromatin immunoprecipitation sequencing (ChIP-seq) data indicates that PLAG1 normally interacts with the *MEG8*:Int2-DMR, although it is unclear if its binding is influenced by DNA methylation [48]. Interestingly, PLAGL2, a homologue of PLAG1, is also predicted to bind the same DMR, as suggested by data from JASPAR CORE 2024—Predicted Transcription Factor Binding Sites [49]. Particularly, PLAGL2 shares 79% identity with PLAG1 in its NH_2-terminal zinc finger domain, suggesting that the zinc finger domain may be involved in recognizing the *MEG8*:Int2-DMR. In humans, ENCODE ChIP-seq data revealed a conserved CTCF binding site within the *MEG8*-DMR [19]. In mice, however, CTCF binds to the *Meg8*-DMR in a non-allele-specific manner in vivo [50]. CTCF (CCCTC-binding factor) is a well-characterized vertebrate protein with eleven zinc fingers, the first ten of which are C2H2-type, similar to those found in PLAG1, while the last one is of C2HC-type [51]. Notably, PLAG1 and CTCF recognize similar consensus sequences, as both bind to G-rich regions.

In the present SRS patients, the truncating *PLAG1* variants map in the last two exons of the gene and should therefore escape the nonsense-mediated decay (NMD) pathway [52]. Also, they likely lead to aberrant PLAG1 proteins, which could influence methylation at the *MEG8*:Int2-DMR because of reduced DNA binding. Indeed, because zinc finger 2 is retained in all these variants, they may dimerize similar to PLAGL1 and exert a dominant-negative effect on the wildtype allele [23]. Consistent with this hypothesis, the single nucleotide deletion (SRS10) and the missense variant (SRS11) in the zinc fingers 6 and 7, that are responsible for specific DNA motif recognition [33], result in *MEG8* hypomethylation. In contrast, the SRS5 variant that contains a C-terminal degron motif and likely results in an unstable aberrant protein is associated with normal *MEG8* methylation [46, 47]. Also, the variants of uncertain pathogenicity are unlikely to disrupt the DNA binding function of PLAG1 and thereby maintain normal *MEG8* methylation. Nevertheless, the mechanism by which reduced PLAG1 binding may interfere with *MEG8* methylation remains to be defined. The absence of methylation defects in the cases with whole gene deletion is consistent with the dominant-negative hypothesis [53].

In SRS16 and the two healthy individuals who scored hypomethylated at the *MEG8*:Int2-DMR according to the MS-MLPA results, further analysis by pyrosequencing showed that this methylation defect was less severe compared to that detected in all the other patients and restricted to a few CpGs located at the 5' part of the DMR, which was shown to be highly variable in a control population. This finding suggests that while MS-MLPA may indicate *MEG8*:Int2-DMR hypomethylation, it does not always reflect the full methylation pattern, and further confirmation using more sensitive and extensive techniques like pyrosequencing or NGS-based technologies like ImprintCap is essential for its accurate assessment.

The observed *MEG8* hypomethylation in the present study suggests that chr14q32 genes have a role in PLAG1-dependent pathogenesis of SRS. Transcription starting from the *MEG3* promoter is crucial for establishing the methylation imprint at the *MEG8*-DMR. In the TS14 cases with *MEG3*: TSS-DMR hypomethylation, the *MEG3* long noncoding RNA is activated and transcription through the *MEG8*:Int2-DMR leads to its hypermethylation [17, 19]. Unfortunately, *MEG3* expression levels could not be assessed in our cases as RNA was not available. However, in all the cases with *PLAG1* mutations, *MEG3* methylation is unaffected, suggesting that alternative molecular mechanisms lead to *MEG8*:Int2-DMR hypomethylation. In a recent study, Baena et al. [19] described a family in which *MEG8* but not *MEG3* exhibits a methylation pattern dependent on the parental origin of a *DLK1* deletion, suggesting an interaction between these two loci. Also, a conserved CTCF binding site is present and therefore an insulator may be formed within the *MEG8*-DMR [19]. Interestingly, several studies indicate a regulatory function of PLAG1 on the *DLK1/MEG3* domain. Declercq et al. [54] demonstrated that targeted PLAG1 overexpression in murine salivary glands induces pleomorphic adenoma-like tumors accompanied by strong upregulation of *Dlk1*. Furthermore, recent transcriptomic profiling of Central Nervous System (CNS) embryonal tumors with *PLAG1* fusions demonstrated upregulation of *DLK1,* supporting the role of PLAG1 in the deregulation of the *DLK1/MEG3* domain [55]. In human hematopoietic stem and progenitor cells (HSPCs) PLAG1 has been shown to activate this locus at the transcriptional level. Specifically, within the *DLK1/MEG3* region on chr14, PLAG1 overexpression induces the expression of multiple imprinted microRNAs, including miR-770, miR-433, miR-127, and miR-370 [56, 57]. However, these reports did not evaluate the methylation of the different DMRs of the *DLK1/MEG3* locus. The *MEG8* DMR overlaps the *MEG8* lncRNA and two clusters of miRNAs and snoRNAs, all of which are deregulated in cancer [58, 59]. It is possible that the disrupted PLAG1 binding to *MEG8* interferes with expression of one or more of these genes. Nevertheless, the molecular mechanisms by which PLAG1 controls the expression of the chr 14 imprinted genes is unknown.

Finally, the normal methylation in the cases with *HMGA2* and *IGF2* variants suggests that *MEG8* works as *PLAG1* target upstream of *HMGA2* and *IGF2* in the *PLAG1–HMGA2-IGF* pathway.

SRS3-SRS5, SRS10-SRS12, SRS15, SRS16 are previously published cases in which the identified *PLAG1* variant was considered the main cause of the SRS phenotype. However, the new molecular analysis on the entire cohort suggests that the VUS present in SRS12 and those of SRS13 and SRS14 may not be damaging. Thus, the variation is unlikely to be causal of the SRS phenotype. Dominant-negative mutations are generally expected to cause more severe phenotypes, because they interfere with the function of the wild-type allele [53]. In the present study, we cannot confidently conclude whether there are significant phenotypic differences between patients carrying *PLAG1* variants associated with *MEG8*-DMR hypomethylation and patients with *PLAG1* variants exhibiting *MEG8*-DMR normal methylation. Within our cohort, only two individuals (SRS13 and SRS16) exhibited a NH-CSS score < 3. They carry a VUS and whole gene deletion, respectively, and both are associated with normal *MEG8* methylation. Unfortunately, the small cohort size limits the possibility to clearly establish a role of *MEG8* methylation in the phenotype of our patients.

Conclusions

The present study identifies *MEG8*:Int2-DMR hypomethylation as a specific epigenetic signature of damaging *PLAG1* variants resulting in stable aberrant proteins, because they likely act in a dominant-negative manner. These findings support a novel pathogenetic mechanism whereby impaired PLAG1 function alters the methylation and possibly the expression of imprinted genes within the chr14q32 region. Furthermore, *MEG8*:Int2-DMR methylation studies might be useful in the future as a functional test for *PLAG1* VUS.

Abbreviations

DMRs	Differentially methylated regions
ImpDis	Imprining disorders
LoM	Loss of methylation
MLID	Multi-locus imprinting disturbances
NH-CSS	Netchine-Harbison clinical scoring system
NMD	Nonsense-mediated decay
PBL	Peripheral blood leukocytes
SRS	Silver-Russell syndrome
SRSp	Silver-Russell syndrome spectrum
SNVs	Single nucleotide variants
TS	Temple syndrome
UPD	Uniparental disomy
VUS	Variant of uncertain significance
ZF	Zinc Finger

Supplementary Information

The online version contains supplementary material available at https://doi.org/10.1186/s13148-025-02024-6.

Supplementary Material 1. Supplementary tables.

Supplementary Material 2. Reduction in MEG8 methylation levels of SRS patients compared to the mean of the controls.

Supplementary Material 3. Pyrosequencing analyses of false positives detected by MS-MLPA.

Supplementary Material 4. ImprintCap results of the MEG8:Int2-DMR methylation in 13 healthy controls.

Supplementary Material 5. Alignment of PLAG1 aberrant proteins.

Supplementary Material 6. UCSC (Human (GRCh37/hg19)) custom track showing the extent of deletions at chromosome 8q12.1 in our cohort.

Acknowledgements

The authors sincerely thank the patients and their families for their valuable participation in this research project. We also thank Sophie Rondeau (Paris), Genevieve Baujat (Paris), Sylvie Rossignol (Strasbourg), Salima El Chehadeh (Strasbourg), Cecile Teinturier (Le Kremlin Bicêtre), Eloise Giabicani (Paris), Jean-Luc Alessandri (Saint Denis La Réunion), Albane Simon (Versailles), Marie-Aliette Dommergues (Versailles), Madeleine Harbison (New York), Godelieve Morel (Saint Denis La Réunion), Bruno Hay Mele (Italy).

Author contributions

Conceptualization, FB, AR, FlCe; investigation, EDA,LP,FrCe,AV,MVC, AS, CG, NT, SR, TE,IN, JRF; writing—draft preparation EDA, FlCe, AR, FB; supervision, FB, AR. All authors have read and agreed to the published version of the manuscript.

Funding

This work was supported by grants from the Associazione Italiana Ricerca sul Cancro (AIRC; IG 2020 ID 24405) and Fondazione Telethon (GMR23T1062) awarded to AR and Italian Ministry of University and Research PRIN 2022B2N2BY awarded to AR and MVC. TE is supported by the Deutsche Forschungsgemeinschaft (EG 115/13–1). ImprintCap experiments were funded with the French Agence Nationale pour la Recherche (ANR) grant no. ANR-22-CE14-0021.

Data availability

The datasets supporting the conclusions of this article are included within the article and its additional files.

Declarations

Ethics approval and consent to participate

The study was approved by the ethical committees of the University of Campania Luigi Vanvitelli (Naples, Italy; approval number: 10423, 5 May 2020), Istituto Auxologico Italiano, Hôpital Trousseau (Paris), Center for Human Genetics and Genome Medicine (Aachen), Hospital General Universitario de Santa Lucía. A written informed consent was obtained from subjects or legals for molecular studies and publication of the data.

Consent for publication

The families agreed for publication by signing an informed consent template.

Competing interests

The authors declare no competing interests.

Author details

[1]Department of Environmental, Biological and Pharmaceutical Sciences and Technologies (DiSTABiF), Università Degli Studi Della Campania "Luigi Vanvitelli", 81100 Caserta, Italy
[2]Department of Genetics, Genomics and Informatics, University of Tennessee Health Science Center, Memphis, TN, USA
[3]Institute of Genetics and Biophysics (IGB) "Adriano Buzzati-Traverso", Consiglio Nazionale Delle Ricerche (CNR), 80131 Naples, Italy
[4]Research Laboratory of Medical Cytogenetics and Molecular Genetics, IRCCS Istituto Auxologico Italiano, 20145 Milan, Italy
[5]Department of Biology, Università Degli Studi Di Napoli "Federico II", Naples, Italy

[6]AP-HP, Hôpital Trousseau, 75012 Paris, France
[7]Center for Human Genetics and Genome Medicine, Medical Faculty, RWTH Aachen University, Aachen, Germany
[8]Servicio de Pediatría, Unidad de Neonatología, Hospital General Universitario de Santa Lucía, Cartagena, Murcia, Spain
[9]Sorbonne Université, Inserm, Centre de Recherche Saint-Antoine, AP-HP, Hôpital Trousseau, 75012 Paris, France

Received: 23 September 2025 / Accepted: 11 November 2025
Published online: 23 November 2025

References

1. Eggermann T, Monk D, De Nanclares GP, Kagami M, Giabicani E, Riccio A, et al. Imprinting disorders. Nat Rev Dis Primers. 2023;9(1):33.
2. Monk D, Mackay DJG, Eggermann T, Maher ER, Riccio A. Genomic imprinting disorders: lessons on how genome, epigenome and environment interact. Nat Rev Genet. 2019;20(4):235–48. https://doi.org/10.1038/s41576-018-0092-0.
3. Court F, Tayama C, Romanelli V, Martin-Trujillo A, Iglesias-Platas I, Okamura K, et al. Genome-wide parent-of-origin DNA methylation analysis reveals the intricacies of human imprinting and suggests a germline methylation-independent mechanism of establishment. Genome Res. 2014;24(4):554–69. https://doi.org/10.1101/gr.164913.113.
4. Mackay DJG, Gazdagh G, Monk D, Brioude F, Giabicani E, Krzyzewska IM, et al. Multi-locus imprinting disturbance (MLID): interim joint statement for clinical and molecular diagnosis. Clin Epigenetics. 2024;16(1):99.
5. Wakeling EL, Brioude F, Lokulo-Sodipe O, O'Connell SM, Salem J, Bliek J, et al. Diagnosis and management of Silver–Russell syndrome: first international consensus statement. Nat Rev Endocrinol. 2017;13(2):105–24.
6. Mackay DJG, Temple IK. Ongoing challenges in the diagnosis of 11p15.5-associated imprinting disorders. Mol Diagn Ther. 2022;26(3):263–72.
7. Sanchez-Delgado M, Riccio A, Eggermann T, Maher ER, Lapunzina P, Mackay D, et al. Causes and consequences of multi-locus imprinting disturbances in humans. Trends Genet. 2016;32(7):444–55. https://doi.org/10.1016/j.tig.2016.05.001.
8. Mackay D, Bliek J, Kagami M, Tenorio-Castano J, Pereda A, Brioude F, et al. First step towards a consensus strategy for multi-locus diagnostic testing of imprinting disorders. Clin Epigenetics. 2022;14(1):143. https://doi.org/10.1186/s13148-022-01358-9.
9. De Crescenzo A, Citro V, Freschi A, Sparago A, Palumbo O, Cubellis MV, et al. A splicing mutation of the HMGA2 gene is associated with Silver–Russell syndrome phenotype. J Hum Genet. 2015;60(6):287–93. https://doi.org/10.1038/jhg.2015.29.
10. Abi Habib W, Brioude F, Edouard T, Bennett JT, Lienhardt-Roussie A, Tixier F, et al. Genetic disruption of the oncogenic HMGA2–PLAG1–IGF2 pathway causes fetal growth restriction. Genet Med. 2018;20(2):250–8. https://doi.org/10.1038/gim.2017.105.
11. Inoue T, Nakamura A, Iwahashi-Odano M, Tanase-Nakao K, Matsubara K, Nishioka J, et al. Contribution of gene mutations to Silver-Russell syndrome phenotype: multigene sequencing analysis in 92 etiology-unknown patients. Clin Epigenetics. 2020;12(1):86. https://doi.org/10.1186/s13148-020-00865-x.
12. Alhendi ASN, Lim D, McKee S, McEntagart M, Tatton-Brown K, Temple IK, et al. Whole-genome analysis as a diagnostic tool for patients referred for diagnosis of Silver-Russell syndrome: a real-world study. J Med Genet. 2022;59(6):613–22. https://doi.org/10.1136/jmedgenet-2021-107699.
13. Weinberg-Shukron A, Youngson NA, Ferguson-Smith AC, Edwards CA. Epigenetic control and genomic imprinting dynamics of the Dlk1-Dio3 domain. Front Cell Dev Biol. 2023;11:1328806.
14. Kagami M, Sekita Y, Nishimura G, Irie M, Kato F, Okada M, et al. Deletions and epimutations affecting the human 14q32.2 imprinted region in individuals with paternal and maternal upd(14)-like phenotypes. Nat Genet. 2008;40(2):237–42.
15. Kagami M, O'Sullivan MJ, Green AJ, Watabe Y, Arisaka O, Masawa N, et al. The IG-DMR and the MEG3-DMR at human chromosome 14q32.2: Hierarchical interaction and distinct functional properties as imprinting control centers. Reik W, editor. PLoS Genet. 2010;6(6):e1000992.
16. Beygo J, Elbracht M, De Groot K, Begemann M, Kanber D, Platzer K, et al. Novel deletions affecting the MEG3-DMR provide further evidence for a hierarchical regulation of imprinting in 14q32. Eur J Hum Genet. 2015;23(2):180–8. https://doi.org/10.1038/ejhg.2014.72.
17. Beygo J, Küchler A, Gillessen-Kaesbach G, Albrecht B, Eckle J, Eggermann T, et al. New insights into the imprinted MEG8-DMR in 14q32 and clinical and molecular description of novel patients with Temple syndrome. Eur J Hum Genet. 2017;25(8):935–45. https://doi.org/10.1038/ejhg.2017.91.
18. Monk D, Morales J, Den Dunnen JT, Russo S, Court F, Prawitt D, et al. Recommendations for a nomenclature system for reporting methylation aberrations in imprinted domains. Epigenetics. 2018;13(2):117–21.
19. Baena N, Monk D, Aguilera C, Fraga MF, Fernández AF, Gabau E, et al. 14q32.2 Novel paternal deletion encompassing the whole DLK1 gene associated with temple syndrome. Clin Epigenetics. 2024;16(1):62.
20. Abi Habib W, Brioude F, Azzi S, Rossignol S, Linglart A, Sobrier ML, et al. Transcriptional profiling at the *DLK1/MEG3* domain explains clinical overlap between imprinting disorders. Sci Adv. 2019;5(2):eaau9425.
21. Hensen K, Van Valckenborgh ICC, Kas K, de Van Ven WJM, Voz ML. The tumorigenic diversity of the three PLAG family members is associated with different DNA binding capacities. Cancer Res. 2002;62(5):1510–7.
22. Voz ML, Agten NS, de Van Ven WJ, Kas K. PLAG1, the main translocation target in pleomorphic adenoma of the salivary glands, is a positive regulator of IGF-II. Cancer Res. 2000;60(1):106–13.
23. Hoffmann A, Ciani E, Boeckardt J, Holsboer F, Journot L, Spengler D. Transcriptional activities of the zinc finger protein Zac are differentially controlled by DNA binding. Mol Cell Biol. 2003;23(3):988–1003.
24. Vado Y, Pereda A, Llano-Rivas I, Gorria-Redondo N, Díez I, Perez De Nanclares G. Novel Variant in PLAG1 in a familial case with silver-russell syndrome suspicion. Genes. 2020;11(12):1461.
25. Meyer R, Begemann M, Hübner CT, Dey D, Kuechler A, Elgizouli M, et al. One test for all: whole exome sequencing significantly improves the diagnostic yield in growth retarded patients referred for molecular testing for Silver–Russell syndrome. Orphanet J Rare Dis. 2021;16(1):42.
26. Brereton RE, Nickerson SL, Woodward KJ, Edwards T, Sivamoorthy S, Ramos Vasques Walters F, et al. Further heterogeneity in Silver–Russell syndrome: PLAG1 deletion in association with a complex chromosomal rearrangement. Am J Med Genet A. 2021;185(10):3136–45.
27. Fernández-Fructuoso JR, De La Torre-Sandoval C, Harbison MD, Chantot-Bastaraud S, Temple K, Lloreda-Garcia JM, et al. Silver Russell syndrome in a preterm girl with 8q12.1 deletion encompassing PLAG1. Clin Dysmorphol. 2021;30(4):194–6.
28. Baba N, Lengyel A, Pinti E, Yapici E, Schreyer I, Liehr T, et al. Microdeletions in 1q21 and 8q12.1 depict two additional molecular subgroups of Silver-Russell syndrome like phenotypes. Mol Cytogenet. 2022;15(1):19.
29. Dong P, Zhang N, Zhang Y, Liu CX, Li CL. Clinical characterization of PLAG1- related Silver-Russell syndrome: a clinical report. Eur J Med Genet. 2023;66(10):104837. https://doi.org/10.1016/j.ejmg.2023.104837.
30. Tse WT, Bass C, Gurney L, Kinning E. Maternally inherited autosomal dominant PLAG-1 related Silver Russell syndrome in a fetus with intra-uterine growth restriction. Prenat Diagn. 2023;43(6):724–6. https://doi.org/10.1002/pd.6364.
31. Wu K, Zhu Y, Zhu Q. Prenatal diagnosis of Silver–Russell syndrome with 8q12 deletion including the PLAG1 gene: a case report and review. Front Genet [Internet]. 2024 May 17 [cited 2024 Dec 17];15. Available from: https://www.frontiersin.org/journals/genetics/articles/https://doi.org/10.3389/fgene.2024.1387649/full
32. Kessler L, Krause J, Kraft F, Amin AK, Fekete G, Lengyel A, et al. Diagnostic Use of Genome Sequencing in Patients With 11p15.5 Imprinting Disorder Features: A Pilot Study. Clin Genet. 2024 Dec 12;
33. Vimercati A, Tannorella P, Guzzetti S, Calzari L, Gentilini D, Manfredini E, et al. Distinguishing genetic alterations versus (epi)mutations in Silver–Russell syndrome and focus on the *IGF1R* gene. J Clin Endocrinol Metab. 2025;110(4):e932–44.
34. Torella A, Ricca I, Piluso G, Galatolo D, De Michele G, Zanobio M, et al. A new genetic cause of spastic ataxia: the p.Glu415Lys variant in TUBA4A. J Neurol. 2023;270(10):5057–63.
35. Garcia M, Juhos S, Larsson M, Olason PI, Martin M, Eisfeldt J, et al. Sarek: A portable workflow for whole-genome sequencing analysis of germline and somatic variants. F1000Research. 2020;9:63.
36. Schubach M, Maass T, Nazaretyan L, Röner S, Kircher M. CADD v1.7: using protein language models, regulatory CNNs and other nucleotide-level scores to improve genome-wide variant predictions. Nucleic Acids Res. 2024;52(D1):D1143–54.
37. Adzhubei IA, Schmidt S, Peshkin L, Ramensky VE, Gerasimova A, Bork P, et al. A method and server for predicting damaging missense mutations. Nat Methods. 2010;7(4):248–9. https://doi.org/10.1038/nmeth0410-248.

38. Ng PC. SIFT: predicting amino acid changes that affect protein function. Nucleic Acids Res. 2003;31(13):3812–4.
39. Cheng J, Novati G, Pan J, Bycroft C, Žemgulytė A, Applebaum T, et al. Accurate proteome-wide missense variant effect prediction with alphamissense. Science. 2023;381(6664):eadg7492.
40. Ioannidis NM, Rothstein JH, Pejaver V, Middha S, McDonnell SK, Baheti S, et al. REVEL: an ensemble method for predicting the pathogenicity of rare missense variants. Am J Hum Genet. 2016;99(4):877–85. https://doi.org/10.1016/j.ajhg.2016.08.016.
41. Richards S, Aziz N, Bale S, Bick D, Das S, Gastier-Foster J, et al. Standards and guidelines for the interpretation of sequence variants: a joint consensus recommendation of the American College of Medical Genetics and Genomics and the Association for Molecular Pathology. Genet Med. 2015;17(5):405–24. https://doi.org/10.1038/gim.2015.30.
42. Riggs ER, Andersen EF, Cherry AM, Kantarci S, Kearney H, Patel A, et al. Technical standards for the interpretation and reporting of constitutional copy-number variants: a joint consensus recommendation of the American College of Medical Genetics and Genomics (ACMG) and the Clinical Genome Resource (ClinGen). Genet Med. 2020;22(2):245–57. https://doi.org/10.1038/s41436-019-0686-8.
43. Szulc NA, Stefaniak F, Piechota M, Soszyńska A, Piórkowska G, Cappannini A, et al. DEGRONOPEDIA: a web server for proteome-wide inspection of degrons. Nucleic Acids Res. 2024;52(W1):W221–32.
44. Sparago A, Verma A, Patricelli MG, Pignata L, Russo S, Calzari L, et al. The phenotypic variations of multi-locus imprinting disturbances associated with maternal-effect variants of NLRP5 range from overt imprinting disorder to apparently healthy phenotype. Clin Epigenetics. 2019;11(1):190. https://doi.org/10.1186/s13148-019-0760-8.
45. Brioude F, Haagmans MA, Mannens M, Netchine I, Alders M, Henneman P, et al. Imprintcap, a powerful NGS-based technology to investigate the molecular background of imprinting disorders. Clin Epigenetics. 2025;17(1):119.
46. Zhao S, Olmayev-Yaakobov D, Ru W, Li S, Chen X, Zhang J, et al. Molecular basis for C-degron recognition by $CRL2^{APPBP2}$ ubiquitin ligase. Proc Natl Acad Sci USA. 2023;120(43):e2308870120.
47. Koren I, Timms RT, Kula T, Xu Q, Li MZ, Elledge SJ. The eukaryotic proteome is shaped by E3 ubiquitin ligases targeting C-terminal degrons. Cell. 2018;173(7):1622-1635.e14. https://doi.org/10.1016/j.cell.2018.04.028.
48. Belew MS, Bhatia S, Keyvani Chahi A, Rentas S, Draper JS, Hope KJ. *PLAG1* and *USF2* co-regulate expression of Musashi-2 in human hematopoietic stem and progenitor cells. Stem Cell Reports. 2018;10(4):1384–97. https://doi.org/10.1016/j.stemcr.2018.03.006.
49. Rauluseviciute I, Riudavets-Puig R, Blanc-Mathieu R, Castro-Mondragon JA, Ferenc K, Kumar V, et al. JASPAR 2024: 20th anniversary of the open-access database of transcription factor binding profiles. Nucleic Acids Res. 2024;52(D1):D174–82.
50. Han X, He H, Shao L, Cui S, Yu H, Zhang X, et al. Deletion of Meg8-DMR enhances migration and invasion of MLTC-1 depending on the CTCF binding sites. Int J Mol Sci. 2022;23(15):8828.
51. Maksimenko OG, Fursenko DV, Belova EV, Georgiev PG. CTCF as an example of DNA-binding transcription factors containing clusters of C2H2-type zinc fingers. Acta Naturae. 2021;13(1):31–46.
52. Lindeboom RGH, Supek F, Lehner B. The rules and impact of nonsense-mediated mRNA decay in human cancers. Nat Genet. 2016;48(10):1112–8. https://doi.org/10.1038/ng.3664.
53. Gerasimavicius L, Livesey BJ, Marsh JA. Loss-of-function, gain-of-function and dominant-negative mutations have profoundly different effects on protein structure. Nat Commun. 2022;13(1):3895.
54. Declercq J, Van Dyck F, Braem CV, Van Valckenborgh IC, Voz M, Wassef M, et al. Salivary gland tumors in transgenic mice with targeted *PLAG1* proto-oncogene overexpression. Cancer Res. 2005;65(11):4544–53.
55. Keck MK, Al-Hussaini M, Amayiri N, Yiadom AAB, Chamyan G, Cheesman E, et al. *PLAG1* fusions define a third subtype of CNS embryonal tumor with *PLAG* family gene alteration. Acta Neuropathol (Berl). 2025;150(1):12.
56. Zhang YW, Cabezas-Wallscheid N. HSCs: slow me down with *PLAG1*. Blood. 2022;140(9):935–6.
57. Keyvani Chahi A, Belew MS, Xu J, Chen HTT, Rentas S, Voisin V, et al. Blood. 2022;140(9):992–1008.
58. Ghafouri-Fard S, Khoshbakht T, Hussen BM, Taheri M, Shojaei S. A review on the role of MEG8 lncRNA in human disorders. Cancer Cell Int. 2022;22(1):285.
59. Krokker L, Patócs A, Butz H. Essential role of the 14q32 encoded miRNAs in endocrine tumors. Genes. 2021;12(5):698.

Publisher's note